Materials and Design 36 (2012) 570–576

Contents lists available at SciVerse ScienceDirect

Materials and Design

journal homepage: www.elsevier.com/locate/matdes

Mechanical characterization of cellulose nanofiber and bio-based epoxy composite

R. Masoodi [a], R.F. El-Hajjar [b,*], K.M. Pillai [a], R. Sabo [c]

[a] Laboratory for Flow and Transport Studies in Porous Media, Department of Mechanical Engineering, University of Wisconsin – Milwaukee, 3200 N. Cramer St., Milwaukee, WI 53211, USA

[b] Engineering Mechanics and Composites Laboratory, Department of Civil Engineering & Mechanics, University of Wisconsin – Milwaukee, 3200 N. Cramer St., Milwaukee, WI 53211, USA

[c] Forest Products Laboratory, United States Department of Agriculture, One Gifford Pinchot Dr., Madison, WI 53726, USA

ARTICLE INFO

Article history:
Received 3 October 2011
Accepted 20 November 2011
Available online 26 November 2011

Keywords:
A. Composites
B. Film and sheet
C. Molding

ABSTRACT

Cellulose nanofibers are one class of natural fibers that have resulted in structures with remarkable mechanical properties. In this study, the cellulose nanofibers are used as reinforcements in the forms of layered films in a bio-derived resin. Assessment of swelling behavior is performed together with an assessment of the tension and fracture behavior. Crack resistance behavior is compared to glass fiber systems and strategies for improving the fracture toughness of "nanopaper" based composites are discussed. Swelling tests indicate the need for constitutive and analysis approaches that account for the swelling response of the developed composites. Increased porosity is observed with higher reinforcement volumes leading to lower than expected mechanical properties. Techniques with higher consolidation pressures are required to improve consolidation processes.

© 2011 Elsevier Ltd. All rights reserved.

1. Introduction

Polymer composites (PCs) are very important materials of recent times. Fiber reinforced PCs that result from combining plastics with reinforcing glass or carbon fibers are lightweight, strong, stiff, and corrosion-resistant. As a result, PCs are increasingly used in several sectors of engineering such as automotive, aerospace, construction, and sports equipment manufacturing. Growing environmental awareness around the world has enhanced interest in the use of environmentally benign materials in engineering. Since the 1990s, natural fiber PCs have emerged as an alternative to glass-reinforced PCs [1]. Natural fiber PCs, such as those made from hemp fiber–epoxy, flax fiber–polypropylene, and china reed–polypropylene, have become particularly attractive in the automotive industries because of their lower cost and lower density, which lead to production of lower-weight components [2].

Other advantages of natural fiber PCs over traditional PCs are economic viability, reduced tool wear during machining operations, enhanced energy recovery, reduced dermal and respiratory irritation, and biodegradability (these advantages have been validated through several lifecycle assessment studies conducted with these materials [2]). According to Directive 2000/53/EC, the European Community enforces member countries to reuse and recover at least 95% of the weight for all end-of-life vehicles by 2015 [3]. Thus, car companies such as Diamler–Chrysler have developed programs to make their automobiles 95% recyclable with the help of natural fiber PCs. For example, Diamler–Chrysler discovered that the use of natural fibers in an engine and transmission casing reduces weight by 10%, lowers the energy needed for production by 80%, while keeping the cost 5% lower than the comparable fiberglass-reinforced component. Consequently, the application of natural fiber PCs of both the thermoplastic and thermoset types is rising in the automobile sector, with average annual growth rates between 10% and 15% [1]. Natural fibers PCs, because of the above mentioned attractive properties, have begun to replace glass or carbon fiber PCs in secondary structural applications such as door panels, package trays, and trunk liners in cars and trucks. Responding to the need for more naturally derived composite materials, research has been focused at synthesizing natural fibers in synthetic and natural resin systems. Abdul Khalil et al. [4] incorporated lignin derived from oil palm biomass waste to improve the thermal stability and mechanical properties of epoxy. Ho and Lau [5] used silk fibers to improve the elastic modulus and impact strength of glass-fiber based composites using less than 1% by weight of additional fibers. The experimental results also indicated an improved strain to failure behavior. Imai et al. [6] used a cellulose film as a carrier for carbon nanotubes and reported improved electrical and mechanical properties. Khalid et al. [7] combined cellulose from empty fruit bunch fiber with a propylene matrix to report improved mechanical properties when using cellulose fillers as compared to using the fibers. The bonding effects of regenerated cellulose natural fibers with epoxy and polyester resins was also studied using a Raman technique [8].

* Corresponding author. Tel.: +1 414 229 3647; fax: +1 414 229 6958.
E-mail address: elhajjar@uwm.edu (R.F. El-Hajjar).

0261-3069/$ - see front matter © 2011 Elsevier Ltd. All rights reserved.
doi:10.1016/j.matdes.2011.11.042

Cellulose nanofibers (CNFs) are one class of natural fibers that have shown remarkable mechanical properties [9–12]. Films or "nanopaper" of cellulose nanofibers have also shown superior mechanical properties [13]. However, the full reinforcing potential of these materials has yet to be realized partly because of issues related to scaling manufacturing processes. Cellulose nanofibers have begun receiving additional attention as a reinforcement material because of reductions in the energy requirements for breaking down cellulose fibers in nanofibers [14]. Awal et al. [15] used cellulose-based nano-composite fibers by an electrospinning process. Recent advances in chemical and mechanical technologies have drastically reduced the energy requirements for producing cellulose nanofibers [13]. To date, no method of forming cellulose nanofibers into pre-forms for liquid composites molding [16] has been reported, and the use of cellulose nanofibers as reinforcements has been limited to layered films and blends of polymers and nanofibers that are either cast or cured, thus limiting the potential for scaling these nanocellulose materials. The composites manufacturing industry has been quick to realize the benefits of using larger parts made of composite materials, however scaling of nanocellulose materials is limited by inadequate understanding of how to process the nanofibers into reinforcements. In addition, it is not clear how the manufacturing processes will affect the properties of the resulting composites.

There have been attempts to produce bio-based PCs using natural fibers and bio-based-resins; however such environment-friendly composites suffer from several limitations such as low mechanical properties due to low strength in reinforcement, and inadequate interfacial strength. Cellulose nanofibers (CNFs) have been shown to have significant potential as a reinforcement, and films cast of filtered nano-fibrillated cellulose were recently observed to have tensile strengths greater than 200 MPa and moduli greater than 14 GPa [12]. However, such films have limited application as polymer reinforcements, and methods for producing scalable cellulose nanofiber reinforcements are absent. In this study, the cellulose nanofibers are used as reinforcements in the forms of layered films in a bio-derived resin. Assessment of swelling behavior is performed together with an assessment of the tension and fracture behavior. Crack resistance behavior is compared to glass fiber systems and strategies for improving the fracture toughness of "nanopaper" based composites are discussed. The porosity in the manufactured composites is measured using an optical imaging method and is correlated to the determined mechanical properties.

2. Manufacturing considerations

2.1. Cellulose nanofiber sheets

Cellulose nanofibers were prepared according to a procedure described by Saito and Isogai [17]. Fully bleached Kraft Eucalyptus fibers were oxidized with sodium hypochlorite using tetramethylpiperidine-1-oxy radical (TEMPO) sodium bromide as catalysts. The TEMPO-mediated oxidation was carried out at pH = 10 and 25 °C for 3 h. The fibers were then thoroughly washed and refined in a disk refiner with a gap of approximately 200 μm. The coarse fibers were separated by centrifuging at 12,000*g*, and the nanofiber dispersion was concentrated to 1% using ultrafiltration. A final clarification step was performed in which the nanofiber dispersed was passed once through an M-110EH-30 Microfluidizer (Microfluidics, Newton, MA) with 200- and 87-μm in series.

The films or sheets of cellulose nanofibers fibers were then formed by ultafiltration of fiber slurries using a 142 mm Millipore ultrafiltration apparatus with polytetrafluoroethylene (PTFE) membranes with 0.1 mm pore sizes (Millipore JVWP14225). Filter paper was placed below the ultrafiltration membranes to provide support. Fiber slurries of approximately 0.2 wt.% were added to the ultrafiltration apparatus to make sheets with a target weight of 1.0 g. After de-watering, individual films were blotted and placed between filter and blotter papers. The films and blotter papers were placed between caul plates with a pressure of approximately 2–3 psi and put in an oven at 50 °C for approximately 3 days. Fig. 1 shows the completed film of cellulose nanofibers that are subsequently used in manufacturing of the epoxy reinforced composite.

A bio-based epoxy is used to reinforce the CNF/Epoxy specimens. The epoxy used in all these experiments is a Super Sap 100/1000 made by Entropy Bio-Resins Co [18]. The bio-based epoxy is an epoxy resin that is made from up of 37% bio-content obtained as co-products of other green industries including wood pulp and bio-fuels production. The resin is classified as a USDA (United States Department of Agriculture) BioPreferred^{SM} Product using ASTM D6866 [19]. The resin has a total calculated biomass of 50%. Using the cellulose nanofiber films as reinforcements, the reinforcements were integrated into the composites. The test specimens were made using a hand lay-up methodology. The resin was degassed using a degassing chamber prior to application for a period of 5 min to allow for the volatiles and voids introduced during the mixing of the hardener and resin to dissipate.

3. Experimental details

3.1. Scanning and transmission electron microscopy

Scanning electron microscopy (SEM) and Transmission electron microscopy (TEM) were performed on the produced specimens to verify the fiber sizes produced and characteristics of the nanofilms. The SEM images were produced using Aqueous nanofiber suspensions of approximately 0.3% were diluted by approximately 10 times in ethanol, and the subsequent suspension was dried on aluminum SEM stubs. The samples were then sputter-coated with gold and imaged with a Zeiss EVO 40 SEM under ultrahigh vacuum conditions (Fig. 2). The TEM images were obtained using the procedure described below. The nanofiber suspension was diluted to approximately 0.001% for transmission electron microscopy, and drops of 5 μL of suspension were dried upon ultrathin carbon films supported by thicker holey carbon films on 600 mesh copper TEM grids. The cellulose nanofibers were then examined using a Philips

Fig. 1. Cellulose nanofiber sheet reinforcement.

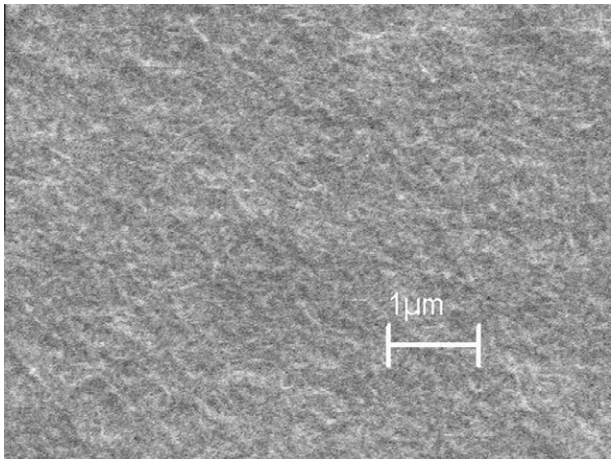

Fig. 2. SEM of cellulose nanofiber sheet reinforcement.

CM120 transmission electron microscope operated at an accelerating potential of 80 keV (Fig. 3).

3.2. Hygro-expansion of CNF reinforcements

The swelling of CNF films in water and epoxy was measured. ASTM D570 [20] was used for guidance in conducting the swelling experiments. An American Scope ME300 metallographic microscope at a magnification of 100× in conjunction with a live capture camera system was used to measure the swelling rates. The microscope was equipped with a measuring software, which was able to measure to a resolution of 5 mm after calibration. The CNF films were cut into narrow strips and placed on a clear slide perpendicular to the slide surface. The initial, pre-swelled, thicknesses of slides were measured using the microscope and software. Then the samples were exposed to water or the bio-based epoxy resin. The photographs of samples were taken every 5 s for a total time of 140 s. The photographs were reviewed to measure the thickness at each specific time. Each test was repeated for five different samples to ensure repeatability of the results.

3.3. Mechanical tests

The testing performed in this section consisted of tension and fracture specimens based on standard specimen geometries (Fig. 4). The standards do not directly address nano-cellulose composites, so the specimens were adapted accordingly as noted. The fracture specimens were as described in ASTM D5528 [21] with the following differences. Two sets of specimens are examined; in one case Fibreglast E-glass (Saertex) are used as reinforcements. The glass fibers are primarily in unidirectional form and had a dry areal weight of 955 g/m^2. They are used for additional stiffness of the fracture test specimens. A thin layer of Teflon film, with length of 50 mm, was placed at one side between the middle layers. The Teflon layer provides the starting point for the crack propagation tests. Two piano hinges were attached on the outer sides of the specimen to enable gripping of the specimens by the test machine. The second set of specimens is identical to those described above with the exception of addition of the CNF layer ahead of the Teflon starter film. A schematic (Fig. 5) of the layup used for the fracture specimens shows the crack starter film going through half the thickness of the specimen. The fracture testing setup is shown in Fig. 6. An optical microscope is used to record the crack growth behavior. The data analysis was performed based on assessment of the mode I strain energy release rate, G_I:

$$G_I = \frac{P^2}{2B}\frac{dC}{da} \tag{1}$$

where P is the applied load to the DCB specimen, C is the compliance, a is the crack size, and B is the specimen width.

The tensile CNF/Epoxy specimens were produced in a cast forming method according to the standard dimensions specified in ASTM D638 [22]. A CNF strip of 11 mm width was placed at the center of the tensile specimen extending to the region of the grips. The average thickness of the CNF film was 0.140 mm. The specimens were left for 24 h at room temperature to cure before removing them from the mold. After the coupons are removed, the edges were machined using a low impact grinding machine and high grit sand paper. The experiments were performed in a displacement control mode at a rate of 2 mm/min. An extensometer was used to measure the strain along a 25.4 mm (1.0 in.) gage section. During the test progress, the crosshead displacement and load were simultaneously recorded. The load was applied using an electromechanical test system with a 97.8 kN (22 kip) capacity. The maximum error of the recorded load was within 22 N (5.0 lb). The same operators using the same test machine tested the entire specimens.

To determining the percentage of porosity within the CNF composite, an imaging based technique was used. This technique involves using a microscopic image and the Hough Transform algorithm [23], which is an algorithm used to detect lines in an image. This program does this by detecting the intensity of pixels in a binary image and then plotting a line based on the pixel values. The modified software uses the Hough Transform [24] formulation incorporated to detect circular objects in a two dimensional image. The program then returns an array of radiuses obtained from each circular object detected. The objective behind this approach in using this detection method is to detect the porosity formations assuming the pores to be shaped like spheres. Fig. 12 validates this by showing the imaging of the porosity in the composite specimen. Transformation to a 3D sphere is made from the 2D images. The radius is used to find the volume of the bubble by the equation of a sphere:

$$V_s = \frac{4}{3}\pi r^3 \tag{2}$$

where V_s is the volume of the sphere and r is the radius. Applying this equation to each element in the array of radiuses an array of volumes is produced. The total volume of the porosity formation is the sum of the individual pores that can be expressed as:

$$V_v = \sum_{i=1}^{n} V_{s,n} = \sum_{i=1}^{n} \frac{4}{3}\pi r_n^3 \tag{3}$$

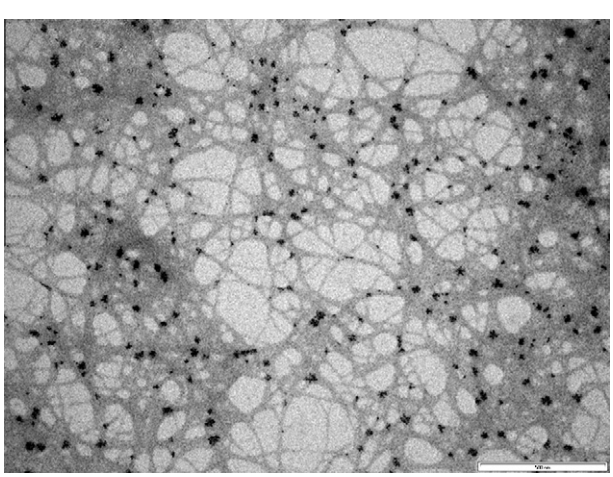

Fig. 3. TEM of cellulose nanofibers.

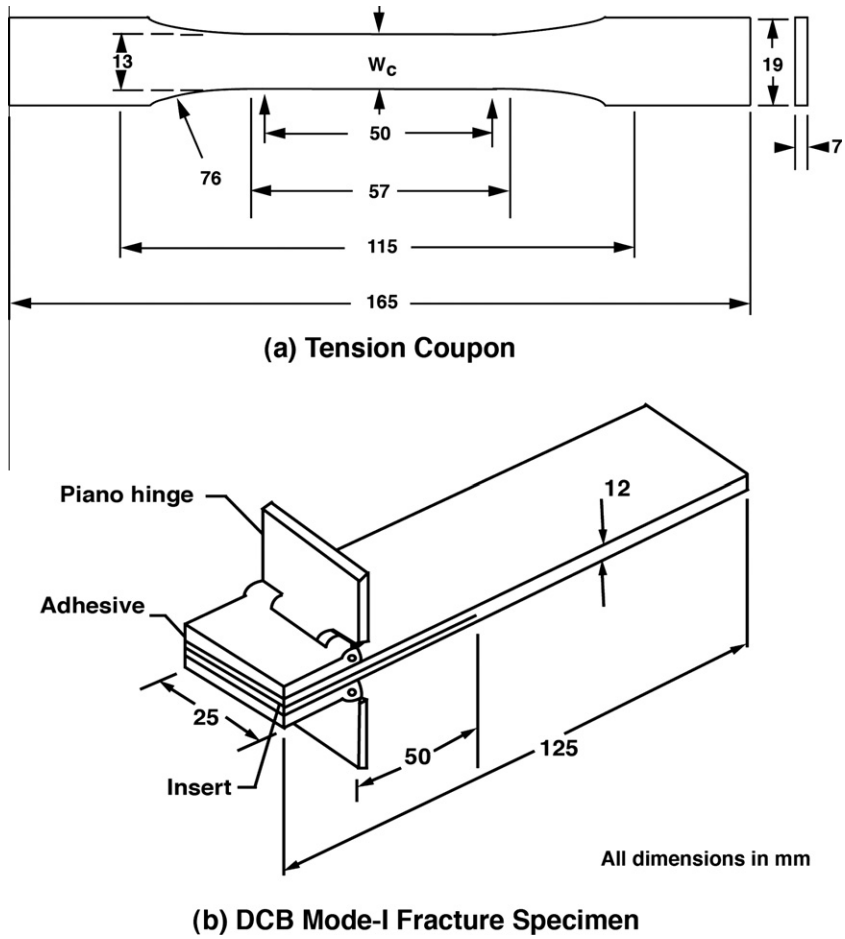

Fig. 4. Schematic of tension and fracture specimens.

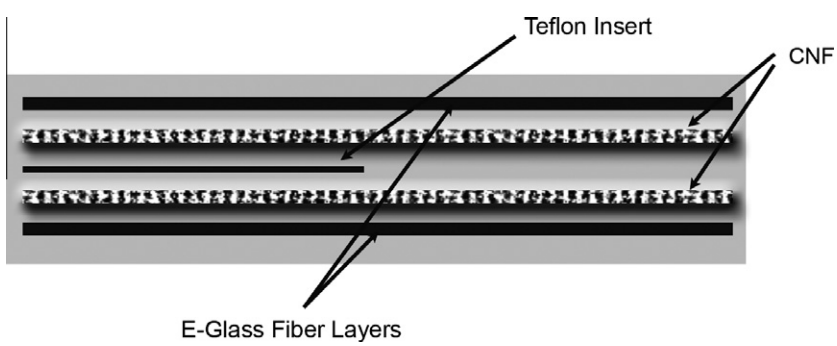

Fig. 5. Schematic of double cantilever beam layup.

In this equation, V_v is the volume of voids and r_n is the radius of the nth element in the array. For determining the porosity, the volume of the interest is estimated by using the thickness of the specimen and the micrograph scan of the surface. The result reported is then a lower bound estimate of the porosity level since the surface scan represents voids at different levels through the thickness. Given that this technique is performed through computer processing, a relationship between the measurement and pixels were predetermined. Since the 2D image already has a length and a width expressed as pixels, the thickness is needed to determine its volume. The thickness was easily obtained by measurement with a caliper gage. The volume being interrogated, is then determined by using these three measurements. The estimated porosity content in percent p, is then expressed as:

$$p = 100\left(\frac{V_v}{V_s}\right) \tag{4}$$

4. Results and discussion

4.1. Swelling tests

Swelling of fibers, used as reinforcing materials, affects the porosity and permeability of fiber mats thus swelling plays an important role in the mold-filling simulations. Swelling reduces pore size and porosity, which results in a reduction in permeability. The thickness growth or swelling measurement results enables mold designers to estimate the porosity and permeability change

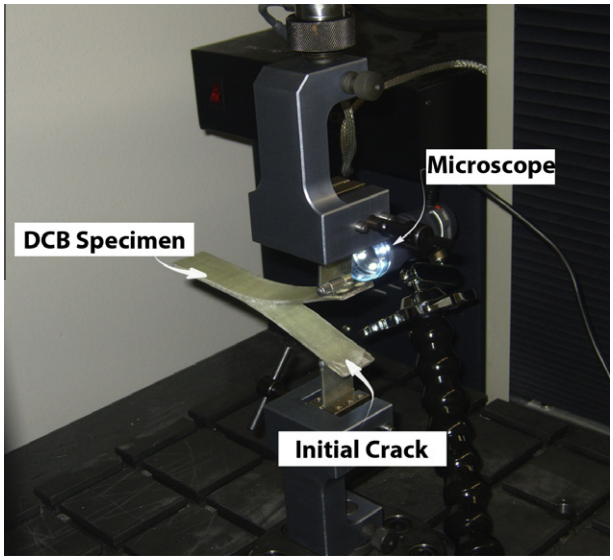

Fig. 6. Test setup for fracture testing.

during the mold filling processes such as LCM. To estimate the swelling of CNF films, a total of five samples were used for each of the three test liquids. The thickness of CNF films increased up to averages of 242% and 159% for water and the bio-derived epoxy after 2 min. This rate of swelling is significant and should be considered in LCM mold-filling simulations as well as the moisture absorption and swelling behavior of final composite products. The swelling observed is also reported in cellulose fibers under moisture and epoxy soaking in LCM processing [16]. The rate of the increase is significant at the initiation of the soaking procedure then stabilizes within a minute of the initiation of the swelling tests. The nonlinear responses for the CNF tests in water and epoxy are shown in Figs. 7 and 8, respectively. Note the variability in the thickness within the sheet, which results in different starting points for each specimen. The main reason for higher swelling rate of CNF films in water is hydrogen bonding of water molecules to the free OH groups present in cellulose molecules.

4.2. Mechanical tests

Fracture testing on CNF sheet reinforced composites panels produced using the hand layup using the sheet type process were examined. Comparisons were made with fiberglass produced with LCM processes and the results showed the increased toughness in fiberglass was driven by the fiber-bridging mechanism. This behavior can be modeled using FE methods such as those using cohesive layered elements [25]. Determination of the cohesive parameters maybe a challenge with the current expense involved in fabricating individual cellulose nanofiber sheets. However, with improved manufacturing techniques this maybe accomplished with miniaturization efforts to reduce the specimen sizes. Fig. 9 shows a typical load versus displacement response for one of the fracture specimens compared to the glass-reinforced specimen showing the fiber-bridging effect. Fig. 10 is a micrograph taken during the crack growth showing the lack of fiber bridging observed in the propagating crack. The crack is retarded manually by not having a self similar growth behavior, but nonetheless the fracture surface does not show significant mechanical interlock between the two surfaces. Increasing the fracture energy required to separate the surfaces across the CNF sheets will result in a larger fracture toughness of the CNF composite. It is also noted that the CNF sheets were not dried prior to manufacturing them into composites, this may result in an imperfect bond during the resin curing process as some of the moisture may have been absorbed from the atmosphere into the natural fibers. Surface modification techniques such as those using 3-aminopropyltriethoxysilane or 3-glycidoxypropyltrimethoxysilane coupling agents may result in improved adhesion between the nanocellulose fibers and the matrix [26]. Application of the surface treatments have to be customized for epoxy resins as these are the most likely to be used. Research in surface treatments can both improve the adhesion and mechanical properties of the nanocellulose composite.

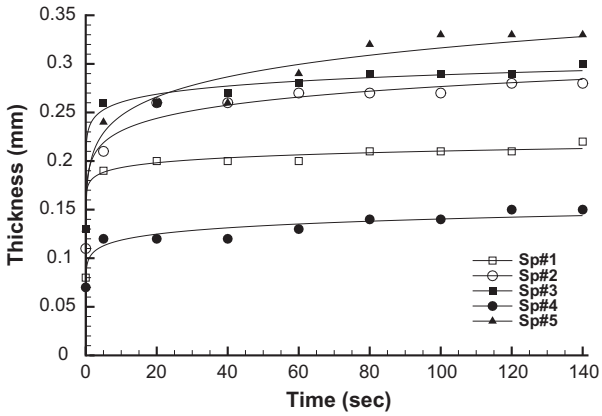

Fig. 7. Swelling responses of CNF sheets in water.

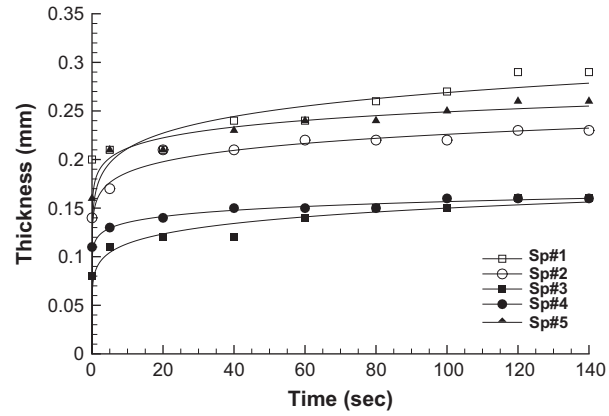

Fig. 8. Swelling responses of CNF sheets in epoxy.

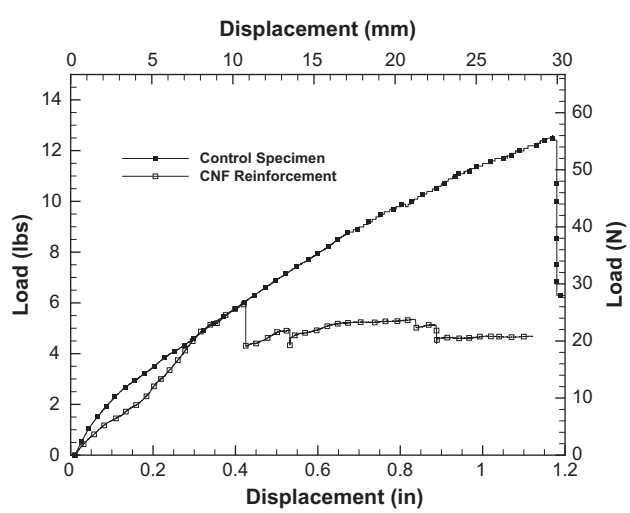

Fig. 9. Fracture resistance behavior of CNF versus glass reinforced epoxy composite.

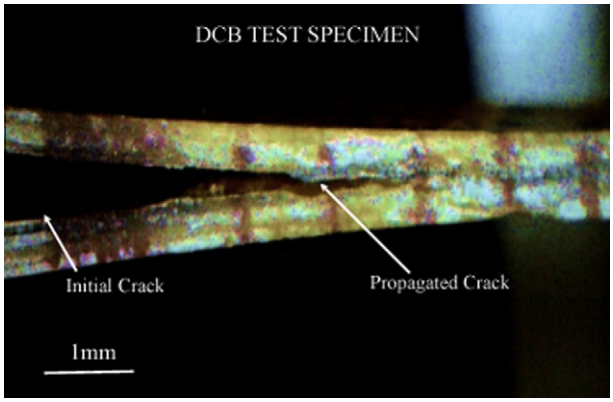

Fig. 10. Crack growth through CNF reinforced composites showing crack front.

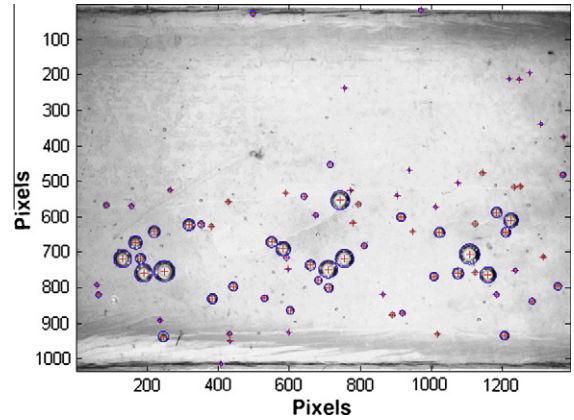

Fig. 12. 3D view of accumulation array of porosity distributions through the thickness.

The tension tests conducted on the CNF reinforced composites show that the addition of small amounts of reinforcing CNF sheets results in improved elastic modulus. The modulus was calculated based on the linear stress strain response using the extensometer data (Fig. 11). Scaling of CNF sheets into a composite system requires an understanding of the mechanical defects that are likely to be generated. Of the defects that can be generated, waviness and porosity are likely to affect the mechanical properties of the manufactured composite. The waviness in this study is not significant due to the size of the specimen considered but this is certainly likely to be a factor when manufacturing larger specimens [27]. The amount of porosity produced in each specimen is found to be very dependent on the amount of reinforcing CNF present in the composite with increasing porosity associated with increased CNF reinforcement. Note that all the specimens were cast from the same batch according to the epoxy vendor specifications so as to avoid batch-to-batch variations in the mechanical properties. The image processing technique applied on one of the specimens is shown in one of the CNF specimens in Fig. 12. It is interesting to note that the voids observed tend to be spherical in nature and occur in different sizes. The porosity levels indicated are likely to be lower bound estimates given that for very small pores, the algorithm is not able to capture the smallest of the pores.

Fig. 13 shows the effect of CNF reinforcement on the modulus and porosity level in the manufactured composite. The higher volume fraction CNF reinforced composite does not yield significantly higher modulus likely due to the increased amount of porosity in the higher volume fraction composite. The higher porosity in the two layer CNF composite is attributed to the increased difficulty for the pores to dissipate from between the two CNF layers compared to the one layer CNF composite. In summary however, compared to the unreinforced resin, an increasing trend is seen with the increasing CNF reinforcement content accounting for the increased porosity levels observed at higher ratios of CNF reinforcing. Fig. 14 shows the modulus as a function of the porosity content for the tension coupons tested. Compared to fiber-based cellulose systems [8] the nanocellulose sheet composites do offer the potential for improved

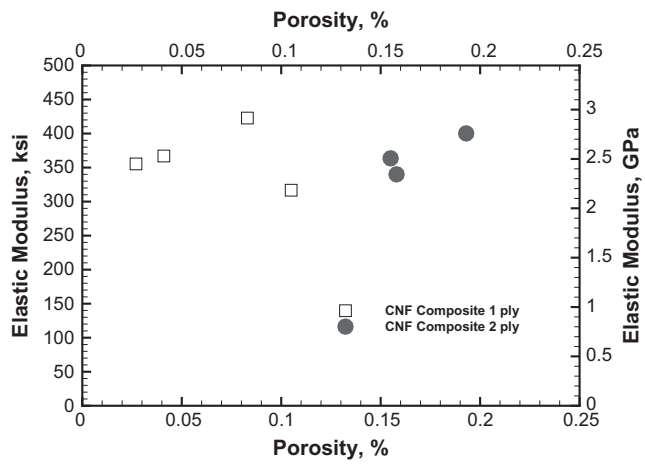

Fig. 13. Relationship of elastic modulus versus porosity levels and CNF reinforcement.

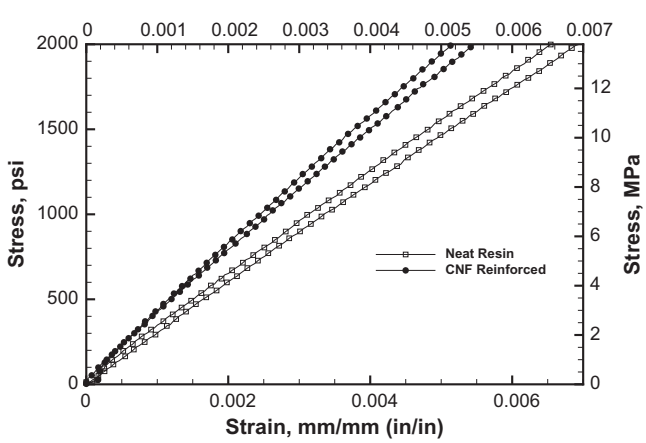

Fig. 11. Stress versus strain response of CNF reinforced and neat resin specimens.

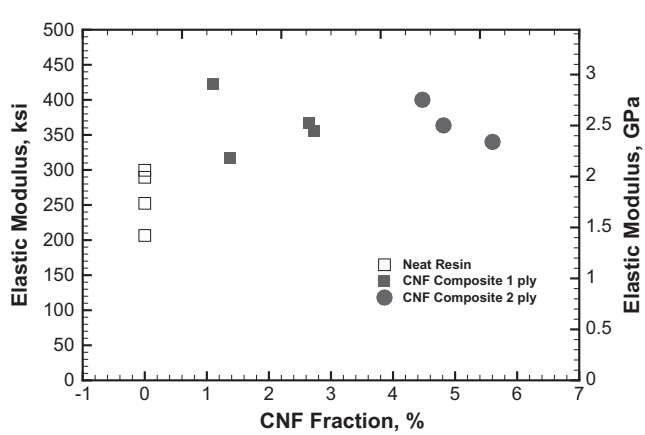

Fig. 14. Relationship between elastic modulus and CNF reinforcement levels.

adhesion with epoxy matrix and resulting improved properties. Simulation of the material behavior for design purposes will require methods to account for crack growth and capturing of the swelling behavior and its effects on the overall design objectives.

5. Conclusions

The current breed of natural-fiber based polymer composites suffer from the drawback of lower strength and fatigue properties compared with carbon or glass fiber-based polymer composites. This study assessed the use of cellulose nanofibers (CNFs) by scaling them into reinforcements in bio-derived polymer composites. The investigation performed reveals the need to enhance the fracture behavior by introducing crack-resistance mechanisms such as fiber bridging. The swelling tests revealed the significant swelling of CNF films in water and epoxy resins. As a future work, more tests with different types of resins will be done to quantify the swelling rate of CNF films in different resins. In addition, characterization of anisotropic swelling will need to be considered. The process modeling effort will be required to link the modeling of CNF distributions to optimize properties. Control of the fiber volume and porosity are likely to result in large improvements in strength, stiffness, and fracture behavior. This will require changes in the processing to increase the consolidation pressure and diffusion of volatiles during the curing process. Moreover, a number of challenges in using cellulose nanofibers for reinforcement still exist, including the dense structure of the fiber networks in these films as well as the swelling of such networks due to liquid absorption during their wetting by resin-like liquids. Future studies will investigate methodologies for improving the fracture toughness of the CNF reinforced composites and methods to lower the void content during manufacturing. This is likely to be challenging if high volume fraction composites are to be manufactured using economical manufacturing processes such as resin transfer molding.

Acknowledgments

The authors would like to thank Jim Beecher and Tom Kuster of the Forest Products Laboratory for performing electron microscopy and Rick Reiner of the Forest Products Laboratory for preparing cellulose nanofibers. The authors would also like to acknowledge the help of the undergraduate research assistants Benton Weibel and Peng Yang at the Flow and Transport Studies in Porous Media and the Experimental Mechanics and Composites Laboratories at the University of Wisconsin – Milwaukee.

References

[1] Brosius D. Natural fiber composites slowly take root. Composites Technology; 2006. <http://www.compositesworld.com/articles/natural-fiber-composites-slowly-take-root.aspx> [01.05.11].
[2] Joshi SV, Drzal LT, Mohanty AK, Arora S. Are natural fiber composites environmentally superior to glass fiber reinforced composites? Composites Part A 2004;35:371–6.
[3] Euro. European Commission Directive 2000/53/EC of the European parliament and the council of 18 September 2000 on end-of-life vehicles, Union OJotE; 2000. p. 9.
[4] Abdul Khalil H, Marliana M, Issam A, Bakare I. Exploring isolated lignin material from oil palm biomass waste in green composites. Mater Des 2011;32(5):2604–10.
[5] Ho M, Lau K. Design of an impact resistant glass fibre/epoxy composite using short silk fibre. Mater Des 2012;35:664–9.
[6] Imai M, Akiyama K, Tanaka T, Sano E. Highly strong and conductive carbon nanotube/cellulose composite paper. Compos Sci Technol 2010;70(10):1564–70.
[7] Khalid M, Ratnam CT, Chuah TG, Ali S, Choong T. Comparative study of polypropylene composites reinforced with oil palm empty fruit bunch fiber and oil palm derived cellulose. Mater Des 2008;29(1):173–8.
[8] Mottershead B, Eichhorn SJ. Deformation micromechanics of model regenerated cellulose fibre-epoxy/polyester composites. Compos Sci Technol 2007;67(10):2150–9.
[9] Lee S, Chun S, Kang I, Park J. Preparation of cellulose nanofibrils by high-pressure homogenizer and cellulose-based composite films. J Indust Eng Chem 2009;15(1):50–5.
[10] Teixeira EM, Pasquini D, Curvelo AAS, Corradini E, Belgacem MN, Dufresne A. Cassava bagasse cellulose nanofibrils reinforced thermoplastic cassava starch. Carbohydr Polym 2009;78:422–31.
[11] Saito T, Hirota M, Tamura N, Kimura S, Fukuzumi H, Heux L, et al. Individualization of nano-sized plant cellulose fibrils by direct surface carboxylation. Biomacromolecules 2009;10:1992–6.
[12] Henriksson M, Burglund LA, Isaksson P. Cellulose nanopaper structures of high toughness. Biomacromolecules 2008;9:1579–85.
[13] Lindström T, Ankerfors M. In: Presented at the 7th international paper and coating chemistry symposium. Hamilton, ON, Canada; June 10–12, 2009.
[14] Siró I, Plackett D. Microfibrillated cellulose and new nanocomposite materials: a review. Cellulose 2010;17:459–94.
[15] Awal A, Sain M, Chowdhury M. Preparation of cellulose-based nano-composite fibers by electrospinning and understanding the effect of processing parameters. Composite Part B 2011;42(5):1220–5.
[16] Masoodi R, Pillai KM. Modeling the processing of natural fiber composites made using liquid composites molding. In: Pilla S editor. Handbook of bioplastics and biocomposites engineering applications. Scrivener-Wiley; 2011.
[17] Saito T, Isogai A. Introduction of aldehyde groups on surfaces of native cellulose fibers by TEMPO-mediated oxidation. Colloids Surf A: Physicochem Eng Aspects 2006;289:219–25.
[18] Entropy SuperSap-100/1000. <http://www.entropyresins.com/sites/default/files/SuperSap-100_1000_TDS.pdf> [01.11.10].
[19] ASTM Standard D6866-11. Standard test methods for determining the biobased content of solid, liquid, and gaseous samples using radiocarbon analysis. ASTM International; 2011.
[20] ASTM Standard D570-98e1. Standard test method for water absorption of plastics. ASTM International; 2010.
[21] ASTM Standard D5528-01e3. Standard test method for mode i interlaminar fracture toughness of unidirectional fiber-reinforced polymer matrix composites. ASTM International; 2007.
[22] ASTM Standard D638-10. Standard test method for tensile properties of plastics. ASTM International; 2010.
[23] Fisher R, Perkins S, Walker A, Wolfart E. Hough transform, <http://www.homepages.inf.ed.ac.uk/rbf/HIPR2/hough.htm> [02.05.10].
[24] Peng T. Detect circles with various radii in grayscale image via Hough Transform. <http://www.mathworks.com> [31.05.11].
[25] El-Hajjar R, Haj-Ali R. Mode-I fracture toughness testing of thick section FRP composites using the ESE(T) specimen. Eng Fract Mech 2005;72(4):631–43.
[26] Lu J, Askeland P, Drzal L. Surface modification of microfibrillated cellulose for epoxy composite applications. Polymer 2008;49(5):1285–96.
[27] El-Hajjar R, Petersen D. Gaussian function characterization of unnotched tension behavior in a carbon/epoxy composite containing localized fiber waviness. Compos Struct 2011;93(9):2400–8.